Nuclear Physics A549 (1992) 550–576
North-Holland

NUCLEAR
PHYSICS A

Meson-exchange currents in electromagnetic transitions of the ^{4}He system*

M. Unkelbach and H.M. Hofmann
Institut für Theoretische Physik, Universität Erlangen-Nürnberg, Erlangen, Germany

Received 15 June 1992

Abstract: In the framework of the refined resonating-group model (RRGM) observables of the photo- and electrodisintegration of ^{4}He into p- and n-channels and those of the corresponding radiative-capture reactions in the giant-resonance energy region are calculated explicitly taking into account meson-exchange currents. The most recent experimental photo- and electrodisintegration cross sections as well as the radiative-capture analyzing powers are well described. Meson-exchange currents are found to make large contributions to the dominant E1 and the M1 transition. Large discrepancies to older calculations are explained.

1. Introduction

Charge independence of the strong interaction and the related concept of isospin had been successful in nuclear physics to a large extent [1]. Nevertheless strict validity of this symmetry became more and more questionable during recent years. This holds true even for the less restrictive principle of charge symmetry requiring invariance only under isospin rotations of 180° instead of arbitrary angles, thus replacing every particle by its mirror partner. Therefore, especially the investigation on mirror reactions is a sensitive tool to test charge symmetry. Neglecting Coulomb effects, the cross sections of mirror reactions are expected to be equal. Of course, the Coulomb force breaks charge symmetry explicitly. But in very light nuclei the effects are supposed to be quite small thus favouring these systems for testing charge symmetry.

Especially the mirror reactions ^{4}He$(\gamma, p)^3$H and ^{4}He$(\gamma, n)^3$He were discussed widely during the past decade since Berman *et al.* [2]) as well as Ward *et al.* [3]) remeasured the ^{4}He$(\gamma, n)^3$He cross section at the beginning of the eighties. Both groups found the cross section to be considerably lower than in all the previous measurements [e.g. refs. [4,5])]. Compared to all existing ^{4}He$(\gamma, p)^3$H cross sections these new data showed a dramatic charge-symmetry breaking in the giant-resonance region. In 1989 Spahn *et al.* did the corresponding electrodisintegration experiment [6]) in which both the ^{4}He$(e, e'p)^3$H and the ^{4}He$(e, e'n)^3$He channels were detected

Correspondence to: Professor Dr. H.M. Hofmann, Institut für Theoretische Physik, Staudtstrasse 7, D-8520 Erlangen, Germany.

* This work has been funded by the German Federal Minister for Research and Technology (BMFT) under contract number 06ER703.

simultaneously thus avoiding different normalization errors. In contrast to the photodisintegration results they found no need for a genuine charge-symmetry breaking. The situation changed when the ^{4}He(γ, p)^{3}H cross sections were remeasured by Bernabei *et al.* [7]) and Feldman *et al.* [8]) in 1988 and 1991, respectively. Similar to the ^{4}He(γ, n)^{3}He channel their new results were considerably lower than the old data points. Compared to the ^{4}He(γ, n)^{3}He data of Berman and Ward these new data no longer showed evidence for a large charge-symmetry breaking. Nevertheless, an experiment measuring both photodisintegration channels simultaneously is still missing.

Although experimentally the question of charge-symmetry violation seems answered for the moment, theoretically the situation is completely unsatisfactory up to now. An older shell-model calculation by Halderson and Philpott [9]) described the old photodisintegration data quite well and therefore overestimates the new one significantly. The same holds true for a coupled-channel resonating-group model (RGM) calculation including Coulomb effects [10]). But at the same time an equivalent RGM calculation using the same potentials and wave functions was able to reproduce the total as well as the differential electrodisintegration cross sections measured by Spahn *et al.* very well [6]). Assuming the new ^{4}He(γ, p)^{3}H and ^{4}He(γ, n)^{3}He data as well as the results of the electrodisintegration experiment to be correct renders the theoretical situation quite strange.

From the theoretical point of view the only difference between an electro- and a photodisintegration experiment lies in the fact that, considering the chosen kinematics, the first is dominated by the longitudinal part of the electromagnetic interaction whereas the second is governed by the transverse part. Searching for mechanisms affecting the transverse but not the longitudinal part of the electromagnetic interaction one is led to the role of meson-exchange currents (MEC). These currents are well known to have only negligible influence on the charge density, but in certain cases to be of great importance in the nuclear current density [e.g. ref. [11])]. Due to the uncertainty of the explicit form of these MEC, especially for phenomenological potentials, on the one hand and the hard calculation on the other, up to now there exists no calculation in the ^{4}He system explicitly including MEC. Rather the MEC are taken into account approximately by the well-known Siegert theorem [12]).

Indeed, the use of Siegert's theorem causes some severe problems, which might be responsible for the failure of the calculations in the case of photodisintegration: First, Siegert's theorem is strictly valid only in the limit $k \to 0$ with k being the momentum transfer of the photon. In the giant-resonance region the energy and momentum transfer is already between 20 and 40 MeV thus questioning the validity of Siegert's theorem. Secondly, all divergence-free currents are neglected. Furthermore, no Siegert theorem exists for magnetic transitions. Although these transitions are quite small and therefore have no influence on the total cross section, they influence other observables like analyzing powers [13]). Considering all this, renders calculations of the photoinduced reactions in ^{4}He including MEC highly desirable.

The usual way to obtain MEC operators is the derivation from the corresponding Feynman diagrams. During the last years this has been done for the most important pion current [11]) as well as for other mesons [14]). However, using nucleon–nucleon potentials not derived from meson-exchange theory, as in RGM models, these currents are useless: As those potentials do not contain an explicit meson exchange, the MEC derived from Feynman rules will not fulfill the continuity equation with the nuclear hamiltonian and therefore lead to an inconsistent description of the electromagnetic interaction with nuclei. On the other hand, calculations using a meson-exchange force like the Bonn potential [15]) are very difficult and are only done for systems with less than four nucleons. Therefore exchange currents for phenomenological potentials are highly desirable.

Several efforts have been undertaken to construct exchange currents for such potentials. Unfortunately, the continuity equation does not determine the MEC uniquely because it gives no information about divergence-free parts of the currents. Therefore additional information is necessary. During the last years especially the approaches of Riska [16]) and Buchmann, Leidemann and Arenhövel [17]) were discussed. They constructed appropriate exchange currents considering the well-known form of the true pion-exchange currents. In this paper we will use a different method derived by Ohta in 1989 [refs. [18,19])]. Starting from gauge invariance he developed a method to determine corresponding exchange currents for arbitrary isospin-dependent, central, spin–orbit and tensor forces.

We organize our paper as follows: In sect. 2 we treat the electromagnetic transition operators, use Ohta's method to derive the two-body operators from our NN potential, sketch the multipole expansion and discuss finally Siegert's theorem, since this discussion is necessary to understand some of our results. Sect. 3 deals with the calculation of the electromagnetic transition matrix elements in the RRGM. In the following section after a short introduction into the ^{4}He wave functions and electromagnetic transition modes, we discuss our results on the photodisintegration cross sections, the radiative-capture observables and the electrodisintregation cross section. Finally, we draw our conclusions in sect. 5. Appendix A contains the explicit calculation scheme for the matrix elements and in appendix B the wave function of the ^{4}He ground state is given.

2. Derivation of interaction operators

2.1. ONE-BODY CURRENTS

Due to the weakness of the electromagnetic interaction compared to the nuclear force, the interaction can be treated in Born approximation. The interaction hamiltonian H_{INT} is given by

$$H_{\mathrm{INT}} = -\frac{1}{c}\int \mathrm{d}^3x\, A_\nu(\boldsymbol{k}, \boldsymbol{x}) j^\nu(\boldsymbol{x}) \tag{1}$$

with k being the momentum transfer of the photon, $A_\mu(k, x)$ the operator of the electromagnetic field and $j^\mu(x) = (c\rho(x), j(x))$ the nuclear current density. The charge density $\rho(x)$ and the spatial current density $j(x)$ are connected by the continuity equation:

$$\nabla \cdot j(x) = \frac{i}{\hbar}[\rho(x), H_N]. \tag{2}$$

This equation is a consequence of the gauge invariance and therefore essential for a consistent description of the electromagnetic interaction in nuclei.

The usual one-body charge-density operator is given by [20-22])

$$\rho^{(1)}(x) = e \sum_{i=1}^{A} \tfrac{1}{2}(1+\tau_{i3})\delta(x-r_i). \tag{3}$$

Here τ_{i3} denotes the third component of the usual Pauli isospin operator acting on the ith nucleon. The r_i are the single-particle coordinates with respect to the center-of-mass system of the A nucleons. This choice is appropriate especially if one describes the nucleon system with translationally invariant models like the RGM.

The one-body current densities are given as the sum of the convection current $j_c(x)$ and the magnetization current $j_s(x)$ [refs. [20-22])]:

$$j^{(1)}(x) = j_c(x) + j_s(x), \qquad j_c(x) = \frac{e}{2m} \sum_{i=1}^{A} \tfrac{1}{2}(1+\tau_{i3})\{p_i, \delta(x-r_i)\}, \tag{4}$$

$$j_s(x) = \frac{e\hbar}{2m} \sum_{i=1}^{A} \tfrac{1}{2}[(1+\tau_{i3})g_{s_p} + (1-\tau_{i3})g_{s_n}]\sigma \times \nabla_i \delta(x-r_i). \tag{5}$$

The p_i are the momentum, the σ_i the Pauli-spin operators of the individual nucleons; g_{s_p} and g_{s_n} denote the spin g-factors of the proton and neutron, respectively.

If one considers the strong nucleonic hamiltonian as a sum of the kinetic energy T and a two-body interaction V,

$$H_N = T + V = \sum_{i=1}^{A} \frac{p_i^2}{2m} + \sum_{i<j}^{A} V_{ij}, \tag{6}$$

it is easy to show that the one-body densities fulfill the continuity equation (2) with the kinetic-energy operator alone. As the nuclear forces contain momentum- and especially isospin-dependent parts, which do not commute with $\rho^{(1)}(x)$ in general, it is evident that the continuity equation is violated with respect to the full nuclear hamiltonian. This demonstrates the necessity of MEC to guarantee self-consistency of the calculation.

2.2. TWO-BODY CURRENTS

As the pion is the lightest meson its exchange currents are the most important ones in a wide range of momentum transfers. Deriving these currents from the

Feynman rules one finds two different parts: a direct term corresponding to a coupling of the photon to the pion directly and a seagull term originating in the coupling to one single nucleon accompanied by the immediate emission of a pion. Due to the importance of the pion-exchange currents we want to investigate effective exchange currents which may be interpreted in terms of a pion exchange.

In order to get the corresponding two-body current operators we use the method of Ohta [18,19]). Starting from gauge invariance he developed a special form of minimal coupling for isospin-dependent potentials. In this manner he derived MEC for arbitrary isospin-dependent, central, tensor and spin-orbit forces. Since the method is explained in ref. [18]) in great detail, we just cite the results. For an arbitrary central force,

$$V_c = \sum_{i<j} \boldsymbol{\tau}_i \cdot \boldsymbol{\tau}_j f_c(r_{ij}) , \tag{7}$$

with $\boldsymbol{r}_{ij} = \boldsymbol{r}_i - \boldsymbol{r}_j$ special minimal coupling yields the following current:

$$j_c(x) = \frac{1}{(2\pi)^6} \sum_{i<j} \int \mathrm{d}^3k' \, \mathrm{d}^3q_{ij} \exp[i\boldsymbol{k}' \cdot (\boldsymbol{R}_{ij} - \boldsymbol{x})] \exp(-i\boldsymbol{q}_{ij} \cdot \boldsymbol{r}_{ij}) \tilde{\boldsymbol{j}}_{ij}(\boldsymbol{k}') , \tag{8}$$

with

$$\tilde{\boldsymbol{j}}_{ij}(\boldsymbol{k}') = \frac{ie}{\hbar} [\boldsymbol{\tau}_i \times \boldsymbol{\tau}_j]_3 \frac{\boldsymbol{q}_{ij}}{\boldsymbol{q}_{ij} \cdot \boldsymbol{k}'} [\tilde{f}_c(|\boldsymbol{q}_{ij} + \tfrac{1}{2}\boldsymbol{k}'|) - \tilde{f}_c(|\boldsymbol{q}_{ij} - \tfrac{1}{2}\boldsymbol{k}'|)] .$$

Here $\tilde{f}_c(q)$ stands for the Fourier transform of $f_c(r)$ and $\boldsymbol{R}_{ij}$ denotes $\frac{1}{2}(\boldsymbol{r}_i + \boldsymbol{r}_j)$. This current fulfills the continuity equation with the original central force V_c by construction.

Similar to the pion-exchange potential an isospin-dependent tensor potential of the form

$$V_t = \sum_{i<j} \boldsymbol{\tau}_i \cdot \boldsymbol{\tau}_j (\boldsymbol{\sigma}_i \cdot \boldsymbol{\nabla}_i)(\boldsymbol{\sigma}_j \cdot \boldsymbol{\nabla}_j) f_t(r_{ij}) , \tag{9}$$

leads to two currents: The first may be interpreted as a seagull current because it results from the minimal coupling to the vertex function:

$$j_s(x) = \frac{e}{\hbar} \sum_{i<j} [\boldsymbol{\tau}_i \times \boldsymbol{\tau}_j]_3 \boldsymbol{\sigma}_i (\boldsymbol{\sigma}_j \cdot \boldsymbol{\nabla}_j) f_t(r_{ij}) \delta(\boldsymbol{x} - \boldsymbol{r}_{ij}) + (i \leftrightarrow j) . \tag{10}$$

The second one corresponds to the direct current:

$$j_d(x) = \frac{1}{(2\pi)^6} \sum_{i<j} \int \mathrm{d}^3k' \, \mathrm{d}^3q_{ij} \exp[i\boldsymbol{k}' \cdot (\boldsymbol{R}_{ij} - \boldsymbol{x})] \exp(-i\boldsymbol{q}_{ij} \cdot \boldsymbol{r}_{ij}) \tilde{\boldsymbol{j}}_{ij}(\boldsymbol{k}') , \tag{11}$$

with

$$\tilde{\boldsymbol{j}}_{ij}(\boldsymbol{k}') = \frac{ie}{\hbar} [\boldsymbol{\tau}_i \times \boldsymbol{\tau}_j]_3 [\boldsymbol{\sigma}_i \cdot (\boldsymbol{q}_{ij} - \tfrac{1}{2}\boldsymbol{k}')][\boldsymbol{\sigma}_j \cdot (\boldsymbol{q}_{ij} + \tfrac{1}{2}\boldsymbol{k}')]$$

$$\times \frac{\boldsymbol{q}_{ij}}{\boldsymbol{q}_{ij} \cdot \boldsymbol{k}'} [f_t(|\boldsymbol{q}_{ij} + \tfrac{1}{2}\boldsymbol{k}'|) - \tilde{f}_t(|\boldsymbol{q}_{ij} - \tfrac{1}{2}\boldsymbol{k}'|)] .$$

In order to derive the effective pion-exchange currents we picked up all terms of our phenomenological potential [23]) with the same functional form as the standard one-pion-exchange potential [11]):

$$V_\pi = -\frac{f^2}{m_\pi} \sum_{i<j} \tau_i \cdot \tau_j (\sigma_i \cdot \nabla_i)(\sigma_j \cdot \nabla_j) \frac{\exp(-\kappa r_{ij})}{\kappa r_{ij}} . \tag{12}$$

In RGM calculations all potentials have to be a superposition of gaussian functions, hence the corresponding terms of our nuclear force are given by

$$V_{ce} = V_0 \sum_{i<j} \tau_i \cdot \tau_j (\sigma_i \cdot \sigma_j) \exp(-\beta r_{ij}^2) , \tag{13}$$

$$V_{te} = V_0 \sum_{i<j} \tau_i \cdot \tau_j [3(\sigma_i \cdot r_{ij})(\sigma_j \cdot r_{ij}) - (\sigma_i \cdot \sigma_j) r_{ij}^2] \exp(-\beta r_{ij}^2) , \tag{14}$$

with β being the width and V_0 the strength parameter of the potential. Applying formula (8) to the central part one immediately gets the following expression:

$$\begin{aligned} j_{ce}(x) = \frac{V_0}{\hbar} \left(\frac{\pi}{\beta}\right)^{3/2} \frac{1}{(2\pi)^6} \sum_{i<j} \int d^3k' \, d^3q_{ij} \exp[ik'(R_{ij} - x)] \exp(-iq_{ij} \cdot r_{ij}) \\ \times ie[\tau_i \times \tau_j]_3 (\sigma_i \cdot \sigma_j) \frac{q_{ij}}{q_{ij} \cdot k'} \\ \times \{\exp[-(q_{ij} + \tfrac{1}{2}k')^2/4\beta] - \exp[-(q_{ij} - \tfrac{1}{2}k')^2/4\beta]\} . \end{aligned} \tag{15}$$

After some manipulations of the term inside the brackets and using the identity

$$\frac{1}{q_{ij} \cdot k'} [\exp(-q_{ij} \cdot k'/4\beta) - \exp(q_{ij} \cdot k'/4\beta)] = -\frac{1}{2\beta} \int_{-1/2}^{1/2} dv \exp(v q_{ij} \cdot k'/2\beta) , \tag{16}$$

the Fourier transform over q_{ij} can be evaluated yielding

$$\begin{aligned} j_{ce}(x) = -\frac{eV_0}{\hbar} \sum_{i<j} \frac{1}{(2\pi)^3} \int d^3k' \exp(ik' \cdot x) [\tau_i \times \tau_j]_3 (\sigma_i \cdot \sigma_j) \\ \times r_{ij} \exp(-\beta r_{ij}^2) \int_{-1/2}^{1/2} dv \exp[-(1 - 4v^2)k'^2/16\beta] \\ \times \exp[ik' \cdot (R_{ij} - v r_{ij})] . \end{aligned} \tag{17}$$

Treating the tensor part is a bit more complicated; one has to rewrite the potential in terms of gradients acting on the exponential function:

$$V_{te} = -\frac{V_0}{4\beta^2} \sum_{i<j} \tau_i \cdot \tau_j [3(\sigma_i \cdot \nabla_i)(\sigma_j \cdot \nabla_j) - (\sigma_i \cdot \sigma_j)(\nabla_i \cdot \nabla_j)] \exp(-\beta r_{ij}^2) . \tag{18}$$

The first term of the sum matches already the form of eq. (9), whereas the second one is coupled in a different manner. But the general procedure can be left

unchanged; the second term is treated analogously to the first one. Applying eq. (10) one finds a term corresponding to the seagull current:

$$j_{se}(x) = -\frac{eV_0}{4\hbar\beta^2} \sum_{i<j} [\tau_i \times \tau_j]_3 \times \{[3\sigma_i(\sigma_j \cdot \nabla_j) - (\sigma_i \cdot \sigma_j)\nabla_j]\delta(x - r_i) \exp(-\beta r_{ij}^2)\} + (i \leftrightarrow j) . \tag{19}$$

The derivation of the term analogous to the direct current is very similar to that of the central current. After inserting the Fourier transform of the gaussian in eq. (11) and carrying out the Fourier transform with the help of eq. (16) one obtains

$$j_{di}(x) = \frac{eV_0}{4\hbar\beta^2} \frac{1}{(2\pi)^3} \int d^3k' \exp(-ik' \cdot x) \times \sum_{i<j} [\tau_i \times \tau_j]_3 [3(\sigma_i \cdot \nabla_i)(\sigma_j \cdot \nabla_j) - (\sigma_i \cdot \sigma_j)(\nabla_i \cdot \nabla_j)] \times r_{ij} \exp(-\beta r_{ij}^2) \int_{-1/2}^{1/2} dv \exp[-(1-4v^2)k'^2/16\beta] \exp[ik'(R_{ij} - v r_{ij})] . \tag{20}$$

Comparing $j_{se}(x)$ as well as $j_{ce}(x)$ and $j_{di}(x)$ with the corresponding well-known true seagull and direct pionic currents [see e.g. ref. [11])] a great similarity is observed. Apart from the different treatment of the scalar parts the only difference occurs in the replacement of the Yukawa by the gaussian functions. Therefore an interpretation of these currents in terms of effective pion-exchange currents is well founded and will be done further on in this paper.

2.3. MULTIPOLE EXPANSION

As the operator $A_\nu(k, x)$ is essentially a plane wave, starting from eq. (1) for the interaction hamiltonian it is convenient to define operators $\mathcal{Q}(k)$ and $\mathcal{T}(k, \mu)$ denoting the longitudinal and the transverse part of the interaction up to some constants:

$$\mathcal{Q}(k) = \int d^3x \, e^{ik \cdot x} \rho(x) , \tag{21}$$

$$\mathcal{T}(k, \mu) = -\frac{1}{c} \int d^3x \, e^{ik \cdot x} e_\mu j(x) . \tag{22}$$

The e_μ stand for the usual spherical unit vectors [24]):

$$e_0 = e_z = \hat{k} , \qquad e_{\pm 1} = \mp\sqrt{\tfrac{1}{2}}(e_x \pm i e_y) . \tag{23}$$

As $\mathcal{T}(k, 0)$ is linearly dependent on $\mathcal{Q}(k)$ via the continuity equation, μ takes only the values 1 and -1.

We take the standard form of the multipole expansion of the plane wave [24]),

$$e^{ik \cdot x} = \sum_{L,M} i^L \sqrt{4\pi(2L+1)} j_L(kx) Y_{LM}(\Omega_x) \mathcal{D}^L_{M0}(\omega_k) , \tag{24}$$

with $j_L(kr)$ denoting the spherical Bessel functions, $Y_{LM}(\Omega_r)$ the spherical harmonics and $\mathscr{D}^L_{MM'}(\omega_k)$ the usual rotation matrices [24]). The triplet of Euler angles is expressed by ω_k. We use the convention of Donnelly and Walecka [22]) and define the longitudinal multipoles as follows:

$$\mathscr{Q}(k)=\sum_{LM} i^L\sqrt{4\pi(2L+1)}\,M_{LM}, \qquad M_{LM}=\int \mathrm{d}^3x\,\rho(x)j_L(kx)\,Y_{LM}(\Omega_x)\,. \quad (25)$$

As there are no two-body contributions to the charge density, the operator $\rho(x)$ is given by the one-body charge density from eq. (3), solely.

The transverse multipoles are treated in the same manner. From Blatt and Weisskopf [25]) we have the expansion

$$\boldsymbol{e}_\mu\,\mathrm{e}^{i\boldsymbol{k}\cdot\boldsymbol{x}}=\sum_{LM} i^L\sqrt{2\pi(2L+1)}$$
$$\times\left(\frac{1}{k}\boldsymbol{\nabla}\times\boldsymbol{L}[j_L(kx)\,Y_{LM}(\Omega_x)]+\mu\boldsymbol{L}[j_L(kx)\,Y_{LM}(\Omega_x)]\right), \quad (26)$$

with $\boldsymbol{L}$ denoting the orbital angular-momentum operator with respect to $\boldsymbol{x}$. Thus the multipole expansion of the transverse part of the electromagnetic interaction can be written as

$$\mathscr{T}(\boldsymbol{k},\mu)=-\sum_{L,M} i^L\sqrt{2\pi(2L+1)}\,(T^{\mathrm{el}}_{LM}+\mu T^{\mathrm{mag}}_{LM})\,, \quad (27)$$

$$T^{\mathrm{el}}_{LM}=\frac{1}{ck}\int \mathrm{d}^3x\,\boldsymbol{j}(\boldsymbol{x})\cdot\boldsymbol{\nabla}\times\boldsymbol{L}[j_L(kx)\,Y_{LM}(\Omega_x)]\,, \quad (28)$$

$$T^{\mathrm{mag}}_{LM}=\frac{1}{c}\int \mathrm{d}^3x\,\boldsymbol{j}(\boldsymbol{x})\cdot\boldsymbol{L}[j_L(kx)\,Y_{LM}(\Omega_x)]\,. \quad (29)$$

The operator $\boldsymbol{j}(\boldsymbol{x})$ is the sum over all one- and two-body currents as described in the previous sections.

2.4. SIEGERT'S THEOREM

As already mentioned in subsect. 2.2, using phenomenological potentials the explicit form of the MEC has been a problem for a long time. Furthermore, calculations including these currents are quite extensive because of their two body nature and their functional form being rather complicated, see subsect. 2.2. On the other hand, including the one-body operators alone is not sufficient. Therefore, one often uses Siegert's theorem, which partly includes MEC. We will sketch the derivation of this theorem briefly because this is necessary to understand some of our results. For a detailed discussion see for instance refs. [26,27]).

The fundamental assumption of Siegert's theorem is the insensitivity of the charge density on MEC, e.g. $\rho(\boldsymbol{x})=\rho^{(1)}(\boldsymbol{x})$. In leading order this holds true for all one-meson-exchange processes because the meson transfers momentum but no

energy [11,16]). In the limit $k \to 0$ the electric (but not the magnetic) multipoles may be written in terms of the divergence of a scalar field:

$$T^{\mathrm{el}}_{LM} \xrightarrow{k\to 0} \frac{i}{k}\frac{L+1}{L}\int \mathrm{d}^3x\, \boldsymbol{j}(\boldsymbol{x})\cdot\boldsymbol{\nabla}[j_L(kx)\,Y_{LM}(\Omega_x)]\,. \tag{30}$$

Integrating by parts and afterwards applying the continuity equation, one obtains a connection between the matrix elements of the electric multipoles and those of the charge density calculated between the intial state $|\lambda_i\rangle$ and the final state $|\lambda_f\rangle$:

$$\begin{aligned}
\frac{1}{c}\frac{L}{L+1}\langle\lambda_f|T^{\mathrm{el}}_{LM}|\lambda_i\rangle &\overset{k\to 0}{=} \frac{i}{ck}\int \mathrm{d}^3x\,\langle\lambda_f|\boldsymbol{j}(\boldsymbol{x})|\lambda_i\rangle\cdot\boldsymbol{\nabla}[j_L(kx)\,Y_{LM}(\Omega_x)] \\
&= -\frac{i}{ck}\int \mathrm{d}^3x\,\langle\lambda_f|\boldsymbol{\nabla}\cdot\boldsymbol{j}(\boldsymbol{x})|\lambda_i\rangle j_L(kx)\,Y_{LM}(\Omega_x) \\
&= \frac{1}{\hbar ck}\int \mathrm{d}^3x\,\langle\lambda_f|[\rho(\boldsymbol{x}),H_{\mathrm{N}}]|\lambda_i\rangle j_L(kx)\,Y_{LM}(\Omega_x) \\
&= \frac{E_i-E_f}{\hbar ck}\int \mathrm{d}^3x\,\langle\lambda_f|\rho(\boldsymbol{x})|\lambda_i\rangle j_L(kx)\,Y_{LM}(\Omega_x) \\
&= -\frac{E_f-E_i}{\hbar ck}\langle\lambda_f|M_{LM}|\lambda_i\rangle\,.
\end{aligned} \tag{31}$$

If one assumes $\rho^{(1)}(\boldsymbol{x})$ to be the complete nuclear-density operator as in Siegert's theorem, the electric-multipole matrix elements of the whole current operator including all MEC can be expressed by the one-body charge-density multipoles.

We would like to draw the reader's attention to the fact that in the derivation the property of $|\lambda_i\rangle$ and $|\lambda_f\rangle$ being eigenstates of H_{N} with energy E_i and E_f is used explicitly. This is no problem in RGM calculations where the wave functions are at least approximately eigenfunctions of the model hamiltonian. However, using wave functions fitted e.g. to the experimental form factors of the fragments, in principle prohibits applying Siegert's theorem.

By construction Siegert's theorem fulfills the continuity equation and includes all MEC with the exception of divergence-free parts. But these parts are negligible for $k \to 0$, because they are purely rotational. Nevertheless, the validity of Siegert's theorem is limited to the small-momentum-transfer region because otherwise eq. (30) no longer holds true. For the magnetic multipoles no similar theorem exists.

3. Wave functions and calculation of the matrix elements

3.1. FORM OF THE WAVE FUNCTIONS

The model we use is the refined resonating-group model (RRGM) initiated by Hackenbroich [28,29]). It is a microscopic model ideally suited to describe reactions

of light nuclei because the model is translationally invariant and therefore the center-of-mass motion is described correctly. As the model is explained in great detail in refs. [28-30]) we only want to give a brief sketch of those aspects necessary to understand the calculation of electromagnetic transitions in the RRGM.

Starting point is the nuclear hamiltonian H_N consisting of kinetic energy and a two-body NN force:

$$H_N = \sum_i \frac{\vec{p}_i^2}{2m} + \sum_{i<j} V_{ij} . \tag{32}$$

As already mentioned the NN potential consists of spin- and isospin-dependent central, tensor and spin-orbit forces of gaussian type, see for instance eqs. (13) and (14); in addition the Coulomb force is included, too. The parameters of the potential are given in ref. [23]); the projection operators in spin and isospin have to be expressed in terms of Pauli spin and isospin matrices.

The cluster wave functions of the bound states coupled to total angular momentum J with parity π consist of a spatial wave function $|\alpha, l, m\rangle$ coupled to total orbital angular momentum l and a spin-isospin part $|\alpha, s, \sigma\rangle$:

$$\psi^{J\pi} = |\kappa, J, j\rangle = \mathcal{A}\bar{\psi}^{J\pi},$$
$$\bar{\psi}^{J\pi} = \sum_{\alpha,l,s} c_\alpha^{l,s,J} (l\, m\, s\, \sigma \,|\, J\, j)|\alpha, l, m\rangle|\alpha, s, \sigma\rangle . \tag{33}$$

The symbol κ stands for all quantum numbers not listed explicitly and α counts the cluster configurations differing from each other by clustering, orbital angular-momentum structure, spin-isospin structure or the cluster width parameters. $\mathcal{A}$ denotes the antisymmetrizer acting on all the nucleons. It consists of the sum over all permutations $\not{p}$ of the A nucleons including their signs:

$$\mathcal{A} = \sum_{\not{p} \in S_A} (-1)^{\not{p}} \not{p} . \tag{34}$$

The spin-isospin functions $|\alpha, s, \sigma\rangle$ are simple products of one-particle spin and isospin spinors. The orbital part $|\alpha, l, m\rangle$ is expressed in Jacobi coordinates and contains gaussians and solid-spherical harmonics. Details may be found in refs. [28-30]).

The two-fragment scattering wave functions with an incoming Coulomb wave in channel τ are given by the expression [23])

$$\psi_\tau^{J\pi} = |\kappa, S_c, L_\tau, J, j\rangle = \sqrt{4\pi(2L_\tau+1)}\, i^{L_\tau} \exp[i\sigma(L_\tau)] \sum_\lambda (\mathrm{Id} - iR)^{-1}_{\tau\lambda}$$
$$\times \mathcal{A}\left\{ \sum_{k=1} \left[\frac{1}{K_k R_k} Y_{L_k}(\Omega_{R_k}) \otimes [\bar{\psi}_k^{J_1^\pi} \otimes \bar{\psi}_k^{J_2^\pi}]^{S_{c_k}} \right]^J \right.$$
$$\left. \times \left(\delta_{\lambda k} F_{L_k}(R_k) + a_{\lambda k} \tilde{G}_{L_k}(R_k) + \sum_m b_{\lambda k m} E_{km}(R_k) \right) \right\} , \tag{35}$$

where $\sigma(L)$ denotes the Coulomb phase shift. The $\bar{\psi}_k^{J_i^\pi}$ are the bound states given in eq. (33) of the fragments in channel k coupled to channel spin S_{c_k}; R_k denotes

the relative motion coordinate. The functions F_{l_k} are regular Coulomb waves, the $\tilde{G}_{L_k}$ are regularized [30]) irregular Coulomb waves and E_{km} are square-integrable functions of the type $R_k^{L_k+1}\exp(\gamma_{km}R_k^2)$ allowing for distortion effects in the interaction region. The elements $a_{\lambda k}$ of the reactance matrix a and the coefficients $b_{\lambda km}$ are fixed by the Kohn–Hulthén variational principle [29]).

Choosing the Coulomb waves as eigenfunctions of the point-Coulomb scattering for the calculated relative energy leads to short-ranged integrals, thus allowing one to expand the scattering waves as gaussians [30]). As a consequence of this expansion all wave functions contain only gaussians and solid-spherical harmonics. For the width parameters we use 5.0, 2.433, 1.2719389, 0.82144556, 0.4447413, 0.2987456, 0.16901745, 0.1185236, 0.080005, 0.05001, 0.0257369, 0.01385, 0.0071429, 0.0038519, 0.0018573, 0.00097261, 0.000561943, 0.00031658, 0.000182973, 0.000101 in units of fm^{-2}.

3.2. CALCULATION OF THE ELECTROMAGNETIC TRANSITION OPERATORS

As already mentioned the electromagnetic transition operators are calculated in Born approximation between the nuclear states described above. The transition operators are split into spherical tensor operators T^{o}_{lm} and $T^{\mathrm{s}}_{r\sigma}$ acting on the configuration and spin part of the wave functions (33):

$$\mathcal{O}_{LM} = \sum_{m,\sigma} (l\, m\, r\, \sigma | L\, M) T^{\mathrm{o}}_{lm} T^{\mathrm{s}}_{r\sigma} . \tag{36}$$

As the coupling between the spin and the orbital operators is different for all the currents, this procedure must be repeated for each current separately. For the longitudinal multipoles M_{LM} nothing has to be done as there is no spin dependence and the orbit part can be calculated directly.

If we choose the short-hand notation

$$\Phi_{LM}(r) = j_L(kr)\, Y_{LM}(\Omega_r) , \tag{37}$$

$$\Delta^J_{LM}(r) = \sum_{M',\nu} (L\, M'\, 1\, \nu | J\, M) \Phi_{LM}(r) e_\nu \cdot p , \tag{38}$$

as well as $\hat{L} = \sqrt{2L+1}$ using eqs. (28) and (29) the multipole operators of the convection current j_{o} can be expressed by

$$\mathcal{O}^{\mathrm{o,el}}_{LM} = \frac{e\hbar}{mc} \frac{1}{\hat{L}} \sum_{i=1}^{A} g_{l_i}\, \mathrm{Id}_{\mathrm{Spin}} [\sqrt{L}\, \Delta^{L+1}_{LM}(r_i) - \sqrt{L+1}\, \Delta^{L-1}_{LM}(r_i)] , \tag{39}$$

$$\mathcal{O}^{\mathrm{o,mag}}_{LM} = i \frac{e\hbar}{mc} \sum_{i=1}^{A} g_{l_i}\, \mathrm{Id}_{\mathrm{Spin}}\, \Delta^{L}_{LM}(r_i) . \tag{40}$$

Similarly one obtains for the magnetization current j_m:

$$\mathcal{O}^{\mathrm{s,el}}_{LM} = -\frac{e\hbar k}{2mc} \sum_{i=1}^{A} g_{s_i} \sum_{M',\nu} (L\, M'\, 1\, \nu | L\, M)\, e_\nu \cdot \sigma_i \Phi_{LM}(r_i) , \tag{41}$$

$$\mathcal{O}^{s\,mag}_{LM} = i\frac{e\hbar k}{2mc}\frac{1}{\hat{L}}\sum_{i=1}^{A} g_{s_i}\sum_{M',\nu}\left[\sqrt{L}\,(L+1\;M'\;1\;\nu|L\;M)e_\nu\cdot\sigma_i\Phi_{L+1\,M'}(r_i)\right.$$
$$\left.-\sqrt{L+1}\,(L-1\;M'\;1\;\nu|L\;M)e_\nu\cdot\sigma_i\Phi_{L-1\,M'}(r_i)\right]. \tag{42}$$

The two-body operators are slightly more complicated. To shorten the notation, we define the following quantities:

$$\Phi 1^J_{LM}(r_i) = \sqrt{\tfrac{4}{3}\pi}\sum_{M'p}(L\,M'\,1\,p|J\,M)j_L(kr_i)Y_{LM'}(\Omega_{r_i})\mathcal{Y}_{1p}(r_{ij}), \tag{43}$$

$$\Phi 2^J_{\tilde{J},LM}(r_i) = 4\sqrt{\tfrac{1}{15}\pi}\sum_F\sqrt{2F+1}\begin{Bmatrix}\tilde{J} & L & 1\\ F & 2 & J\end{Bmatrix}$$
$$\times\sum_{M'f}(L\,M'\,F\,f|J\,M)j_L(kr_i)Y_{LM'}(\Omega_{r_i})$$
$$\times\sum_{pq}(1\,p\,Q\,q|F\,f)\mathcal{Y}_{1p}(r_{ij})\mathcal{Y}_{Qq}(r_{ij}), \tag{44}$$

$$\xi_{ij}(v) = \exp(-\beta r_{ij}^2)\exp[-(1-4v^2)k^2/16\beta], \tag{45}$$

$$\rho_{ij}(v) = R_{ij} - vr_{ij}, \tag{46}$$

with $\mathcal{Y}_{LM}(r)$ denoting the solid-spherical harmonics. The simplest two-body operator results from the central current j_{ce}:

$$\mathcal{O}^{ce\,el}_{LM} = -i\frac{eV_0}{\hbar c}\frac{1}{\hat{l}}\sum_{i<j}[\tau_i\times\tau_j]_3(\sigma_i\cdot\sigma_j)$$
$$\times\int_{-1/2}^{1/2}dv\,\xi_{ij}(v)\{\sqrt{L}\,\Phi 1^L_{L+1\,M}(\rho_{ij}(v)) - \sqrt{L+1}\,\Phi 1^L_{L-1\,M}(\rho_{ij}(v))\}, \tag{47}$$

$$\mathcal{O}^{ce\,mag}_{LM} = \frac{eV_0}{\hbar c}\sum_{i<j}[\tau_i\times\tau_j]_3(\sigma_i\cdot\sigma_j)\int_{-1/2}^{1/2}dv\,\xi_{ij}(v)\Phi 1^L_{LM}(\rho_{ij}(v)). \tag{48}$$

The seagull current j_{se} needs a recoupling, because the spin and the orbit part of the operator are mixed. Since this recoupling is straightforward but lengthy we just give the result:

$$\mathcal{O}^{se\,el}_{LM} = i\frac{eV_0}{\hbar c}\frac{3}{2\beta}\frac{1}{\hat{L}}\sum_{i<j}[\tau_i\times\tau_j]_3\sum_{r=1,2\sigma}(-1)^r\sqrt{2r+1}\,[\sigma_i\otimes\sigma_j]_{r\sigma}$$
$$\times\sum_{C,M'}\sqrt{2C+1}\,(C\,M'\,2\,\sigma|L\,M)\exp(-\beta r_{ij}^2)$$
$$\times\left(\begin{Bmatrix}L & L+1 & 1\\ 1 & r & C\end{Bmatrix}\sqrt{L}\,\Phi 1^C_{L+1\,M'}(r_i) - \begin{Bmatrix}L & L-1 & 1\\ 1 & r & C\end{Bmatrix}\sqrt{L+1}\,\Phi 1^C_{L-1\,M'}(r_i)\right)$$
$$+(i\leftrightarrow j), \tag{49}$$

$$\mathcal{O}^{se\,mag}_{LM} = \frac{eV_0}{\hbar c}\frac{3}{2\beta}\sum_{i<j}[\tau_i\times\tau_j]_3\sum_{r=1,2\sigma}(-1)^r\sqrt{2r+1}\,[\sigma_i\otimes\sigma_j]_{r\sigma}$$
$$\times\sum_{C,M'}\sqrt{2C+1}\,(C\,M'\,2\,\sigma|L\,M)\exp(-\beta r_{ij}^2)$$
$$\times\begin{Bmatrix}L & L & 1\\ 1 & r & C\end{Bmatrix}\Phi 1^C_{LM'}(r_i)+(i\leftrightarrow j). \tag{50}$$

The direct current $j_{\rm di}$ is the most difficult one. Applying the gradients one finds five expressions of different structure. Three of them have an additional k-dependence besides the plane wave, therefore being of higher order in k than the two others. As we want to restrict ourselves to momentum transfers lower than 80 MeV/c, we may neglect these terms with respect to the two leading ones. After the multipole expansion and a necessary recoupling of spin and orbit parts one is led to the following four operators:

$$\mathcal{O}^{\rm dif^{el}}_{LM} = -i\frac{eV_0}{\hbar c}\frac{1}{\hat{L}}\frac{12\sqrt{5}}{\beta}\sum_{i<j} i[\boldsymbol{\tau}_i\times\boldsymbol{\tau}_j]_3\sum_{\sigma}[\boldsymbol{\sigma}_i\otimes\boldsymbol{\sigma}_j]_{2\sigma}$$
$$\times\sum_{C,M'}\sqrt{2C+1}\,(C\,M'\,2\,\sigma|L\,M)\int_{-1/2}^{1/2}\mathrm{d}v\,\xi_{ij}(v)$$
$$\times\left(\begin{Bmatrix} L & L+1 & 1\\ 1 & 2 & C\end{Bmatrix}\sqrt{L}\,\Phi 1^{C}_{L+1\,M'}(\boldsymbol{\rho}_{ij}(v))\right.$$
$$\left.-\begin{Bmatrix} L & L-1 & 1\\ 1 & 2 & C\end{Bmatrix}\sqrt{L+1}\,\Phi 1^{C}_{L-1\,M'}(\boldsymbol{\rho}_{ij}(v))\right), \tag{51}$$

$$\mathcal{O}^{\rm dif^{mag}}_{LM} = -\frac{eV_0}{\hbar c}\frac{12\sqrt{5}}{\beta}\sum_{i<j}[\boldsymbol{\tau}_i\times\boldsymbol{\tau}_j]_3\sum_{\sigma}[\boldsymbol{\sigma}_i\otimes\boldsymbol{\sigma}_j]_{2\sigma}$$
$$\times\sum_{C,M'}\sqrt{2C+1}\,(C\,M'\,2\,\sigma|L\,M)\int_{-1/2}^{1/2}\mathrm{d}v\,\xi_{ij}(v)$$
$$\times\begin{Bmatrix} L & L & 1\\ 1 & 2 & C\end{Bmatrix}\Phi 1^{C}_{LM'}(\boldsymbol{\rho}_{ij}(v)), \tag{52}$$

$$\mathcal{O}^{\rm dif\,II^{el}}_{LM} = -i4\sqrt{6}\frac{eV_0}{\hbar c}\frac{1}{\hat{L}}\sum_{i<j}[\boldsymbol{\tau}_i\times\boldsymbol{\tau}_j]_3\sum_{\sigma}[\boldsymbol{\sigma}_i\otimes\boldsymbol{\sigma}_j]_{2\sigma}$$
$$\times\sum_{C,M'}\sqrt{2C+1}\,(C\,M'\,2\,\sigma|L\,M)\int_{-1/2}^{1/2}\mathrm{d}v\,\xi_{ij}(v)$$
$$\times\{\sqrt{L}\,\Phi 2^{C}_{L,L+1\,M'}(\boldsymbol{\rho}_{ij}(v))-\sqrt{L+1}\,\Phi 2^{C}_{L,L-1\,M'}(\boldsymbol{\rho}_{ij}(v))\}, \tag{53}$$

$$\mathcal{O}^{\rm dif\,II^{mag}}_{LM} = -4\frac{eV_0}{\hbar c}\sum_{i<j}[\boldsymbol{\tau}_i\times\boldsymbol{\tau}_j]_3\sum_{\sigma}[\boldsymbol{\sigma}_i\otimes\boldsymbol{\sigma}_j]_{2\sigma}$$
$$\times\sum_{C,M'}\sqrt{2C+1}\,(C\,M'\,2\,\sigma|L\,M)$$
$$\times\int_{-1/2}^{1/2}\mathrm{d}v\,\xi_{ij}(v)\Phi 2^{C}_{L,LM'}(\boldsymbol{\rho}_{ij}(v)). \tag{54}$$

The calculation of the matrix elements of these operators,

$$\langle J'\,j'|\mathcal{A}\mathcal{O}_{LM}|J\,j\rangle, \tag{55}$$

is done in two steps: First the spin-isospin matrix element is evaluated for every permutation. Since the spin-isospin functions are simple products of one-particle spinors this can be done easily using the well-known SU(2) technics. In the end all

spin-isospin matrix elements giving the same coordinate-space matrix elements due to the cluster symmetry of the $|\alpha lm\rangle$ are summed up, see ref. [30]).

The most complicated step is the calculation of the coordinate-space matrix elements. The matrix elements of all operators are of the general form (except for the convection current, which contains additional gradients)

$$I = \langle \alpha_f, l_f, m_f | \not{\Phi}_{LM}(\boldsymbol{\rho}_{ij}(v)) \exp(-\beta r_{ij}) \prod_{N=1}^{N_0} \mathcal{Y}_{L_N M_N}(\boldsymbol{r}_{ij}) | \alpha_i, l_i, m_i \rangle . \qquad (56)$$

For the direct and central current operators one has to adjust the number N_0 of the solid-spherical harmonics to 1 or 2, see eqs. (47), (48) and (51)-(54). For the seagull terms (49) and (50) N_0 equals 1; to obtain the two parts one puts $v = -\frac{1}{2}$ ($\boldsymbol{\rho}_{ij} = \boldsymbol{r}_i$) and $v = \frac{1}{2}$ ($\boldsymbol{\rho}_{ij} = \boldsymbol{r}_j$), see eq. (46). The orbital matrix elements of the one-body spin operators (41) and (42) are calculated with $v = -\frac{1}{2}$, $\beta = 0$ and $N_0 = 0$. The calculation scheme for the explicit evaluation of the coordinate-space matrix elements of type (56) is given in appendix A together with the corresponding result for the convection-current operators (39) and (40). With the help of the expressions in appendix A we are able to calculate all electromagnetic transition operators.

4. Results and discussion

4.1. ELECTROMAGNETIC TRANSITIONS IN THE ^{4}He SYSTEM

In this section we want to discuss our results on electromagnetic transitions between the ^{4}He ground state and two-fragment scattering channels. In the case of photodisintegration there exist $^4\mathrm{He}(\gamma, \mathrm{p})^3\mathrm{H}$, $^4\mathrm{He}(\gamma, \mathrm{n})^3\mathrm{He}$ and $^4\mathrm{He}(\gamma, \mathrm{d})^2\mathrm{H}$ reaction channels, whereas the radiative-capture processes are just the inverse reaction. In the electrodisintegration the corresponding (e, e'X) channels are taken into account.

As far as charge-symmetry breaking is concerned especially the p- and n-channels are of interest. Furthermore, due to the isosinglet structure of the deuteron and the ^{4}He ground state there are no direct MEC contributions in the dd channels, because all two-body currents are isovector operators, see sect. 3. Therefore in our calculation we found only small MEC corrections in these channels caused by coupling to the p- and n-channels. Since the dd channels have already been discussed by Wachter *et al.* [31]) in great detail we restrict ourselves to the p- and n-channels in this paper.

In the present calculation we used the same semi-realistic potential as in refs. [10,31]). Therefore we were able also to take the same wave functions for the ground and the scattering states, thus making these calculations directly comparable. In this paper we only used the ground-state wave function with 12% D-wave admixture, which has the following structure:

$$\begin{aligned} |^4\mathrm{He}\rangle = |\psi^{0+}\rangle = \mathcal{A}_4\{ & \alpha[^3\mathrm{H}\text{-}\mathrm{p}]^{L_r=0,S_c=0} \\ & + \beta[^3\mathrm{He}\text{-}\mathrm{n}]^{L_r=0,S_c=0} + \gamma[^2\mathrm{H}\text{-}\mathrm{d}]^{L_r=0,S_c=0} \\ & + \delta[^2\mathrm{H}\text{-}\mathrm{d}]^{L_r=2,S_c=2}\} . \end{aligned} \qquad (57)$$

The D-state probability of 12% originates solely from the ^{2}H–d structure with $L_r = 2$, because none of the ^{3}H, ^{3}He or ^{2}H fragments contains any D-wave. The detailed structure of the bound state is given in appendix B. The scattering states have the same structure but with a continuum instead of a bound function between the fragments.

In fig. 1 we compare the experimental with the calculated thresholds in the ^{4}He system with respect to the ^{3}H–p breakup energy. On the one hand the dd threshold is too low, causing some minor problems at very low energies. On the other hand, the ^{4}He ground state is too weakly bound, a problem common to all calculations using two-body NN potentials without adjustable parameters. Keeping the channel energy E_c fixed means the calculated momentum transfer k_m is too small compared to the experimental value k_{ex}. Since the electromagnetic matrix elements contain powers of k this leads to a wrong energy behavior of all the observables. To correct for this we replace the model value k_m by the experimental value k_{ex}.

In the calculation of the observables we take into account E1/C1, M1 and E2/C2 transitions. In the p- and n-channels these transitions are related to the $^1P_1$ and $^3P_1$ channels (E1/C1), the $^3S_1$ and $^3D_1$ channels (M1) and the $^1D_2$ and $^3D_2$ channels (E2/C2; notation $^{2S_c+1}L_S$). As expected, the $^1P_1$ transition is the strongest one by a considerable margin, followed by $^3P_1$, $^1D_2$ and $^3D_1$. The other transitions are found to be nearly negligible.

In the following subsections we will discuss the results of three different calculations:

- impulse approximation: one-body convection and magnetization currents only.
- Siegert approximation: Siegert operator used to calculate the electric transitions, impulse approximation used in magnetic ones.
- full calculation: all one- and two-body currents taken into account.

4.2. PHOTODISINTEGRATION CROSS SECTIONS

In figs. 2 and 3 the calculated total ^{4}He photodisintegration cross sections into p- and n-channels are compared to experimental data. In both channels the large discrepancies between the older and the more recent measurements are striking; the new experimental cross sections are about 30–40% smaller than the older ones.

Considering the results of the various calculations one first recognizes the large difference between the full calculation including MEC (full line) and the impulse approximation (dotted line). This indicates large contributions of two-body currents. Because the $^1P_1$ transition is the most dominant one and gives nearly 98% of the total cross section, it is interesting to take a detailed view of the contributions of the different currents. This is done in table 1. The most important mesonic contribution comes from the central current $\mathcal{O}^{ce}$. The seagull and the direct terms are of vector or tensor structure in spin space. Hence, both transitions are forbidden between the $^1P_1$ scattering-state and the dominant $^1S_0$ ground-state configuration,

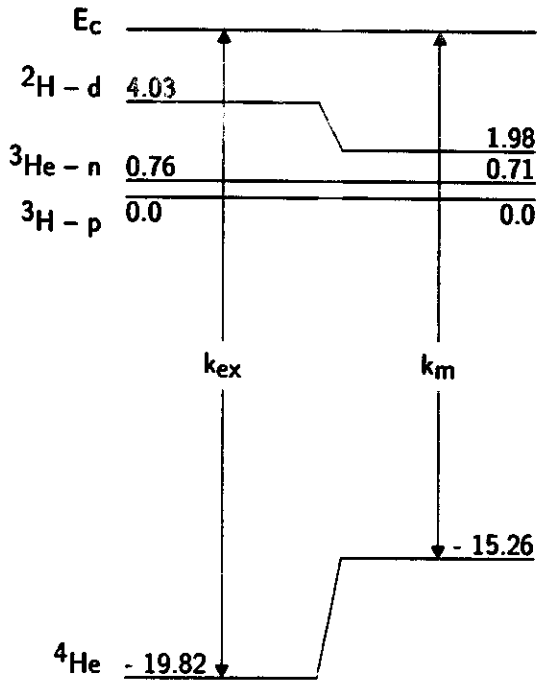

Fig. 1. Thresholds in the ^{4}He system compared to the ^{3}H-p threshold: on the left-hand side the experimental values, on the right-hand side those calculated using the semi-realistic NN potential; all energies in MeV.

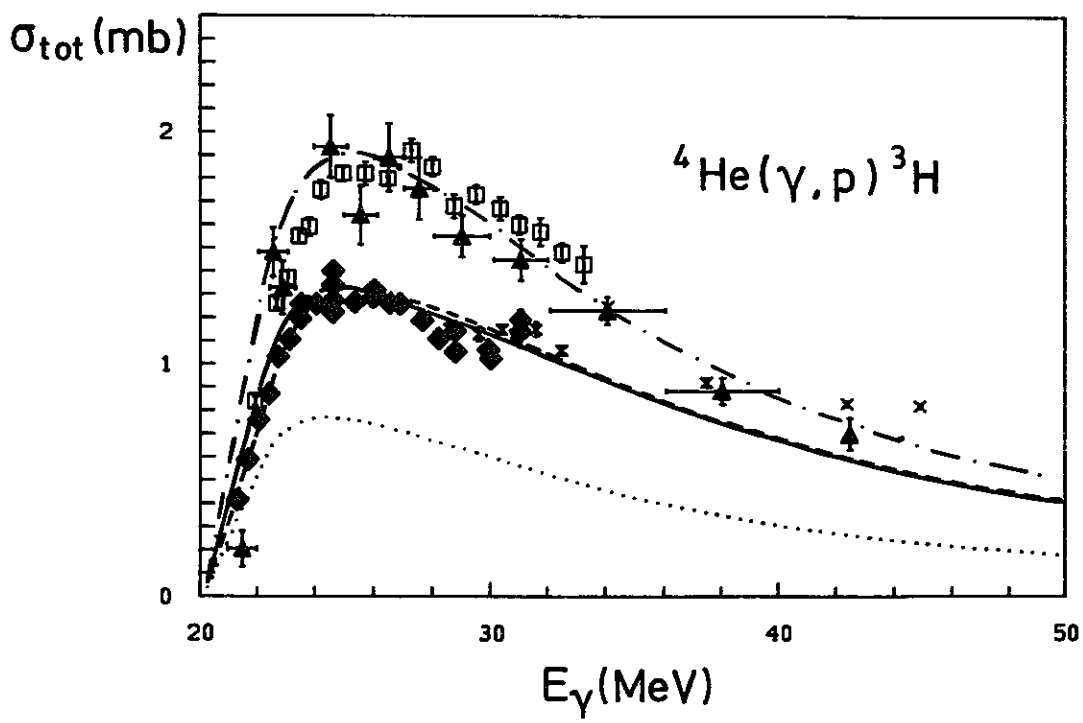

Fig. 2. Total cross section of the reaction ^{4}He(γ, p)^{3}H. Full line: full calculation; dashed line: Siegert's approximation; dotted line: impulse approximation; dash-dotted line: Wachter *et al.* (Siegert) [10]. Data: (square) Meyerhof (1970) [32]; (triangle) Gorbunov (1968) [33]; (diamond) Feldman (1990) [8]; (cross) Bernabei (1988) [7].

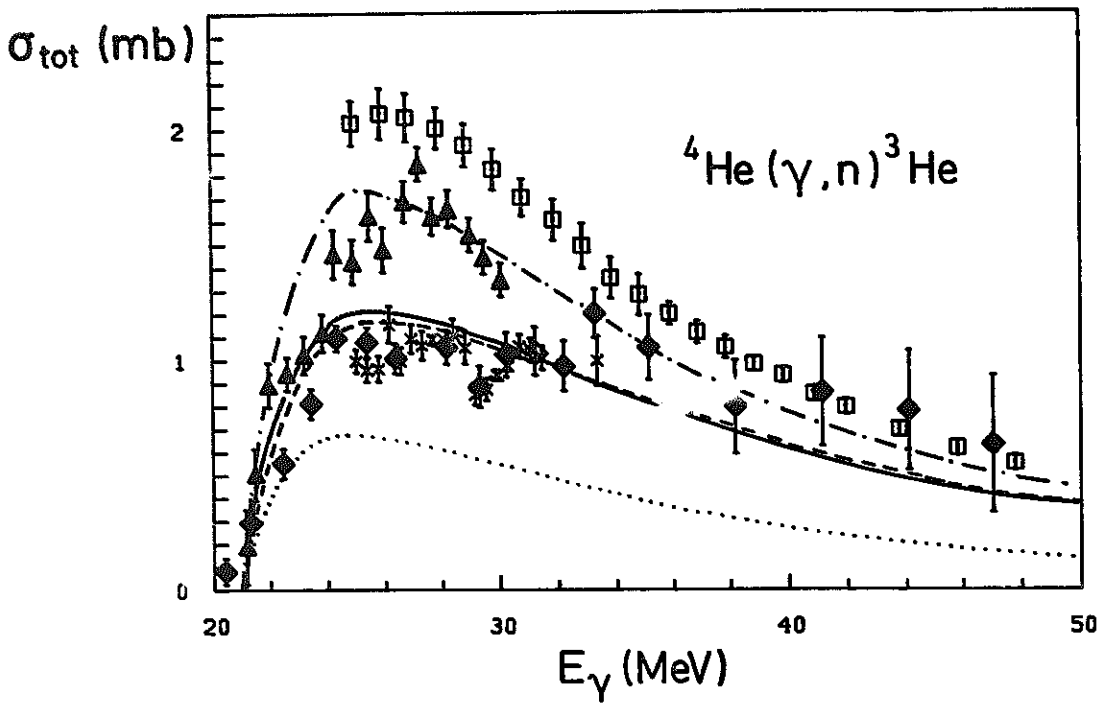

Fig. 3. As in fig. 2 but for the reaction ^{4}He(γ, n)^{3}He. Data: (square) Malcolm (1973) [4]; (triangle) Irish (1975) [5]; (diamond) Berman (1980) [2]; (cross) Ward (1981) [3].

except for small channel-coupling effects. Transitions into the small $^5D_0$ ground-state component are allowed, thus being sensitive on the D-state admixture.

The most remarkable result is the large discrepancy between the full calculation with MEC (full line) and the old Siegert calculation of Wachter *et al.* [10]) (dash-dotted line). As already mentioned, this calculation was done using the same NN potential and the same wave functions as in the present calculation. At a first glance one might conclude that large divergence-free parts of meson-exchange currents occur, which are not included in Siegert's theorem. Although unexpected at this order of magnitude such contributions might be possible because of the quite large momentum transfer of 20–50 MeV/c. But this is not the case: Putting the momentum transfer k equal to 0 by hand, we found the difference between the matrix elements still

TABLE 1

Contributions of the different operators in the $^1P_1$ transition of the reaction ^{4}He(γ, p)^{3}H at $E_{c.m.} = 4.5$ MeV normalized to $\mathcal{O}^o$

$\mathcal{O}^o$	1.000
$\mathcal{O}^s$	≈0.0
$\mathcal{O}^{ce}$	0.196
$\mathcal{O}^{se}$	0.179
$\mathcal{O}^{dil,II}$	−0.054

remains. This contradicts Siegert's theorem as described in sect. 2, because divergence-free currents vanish in this limit.

The explanation of the discrepancy lies in the application of Siegert's theorem itself in the older calculation. As sketched in subsect. 2.4 Siegert's theorem connects the matrix elements of the electric transitions with those of the charge density via

$$\frac{1}{c}\frac{L}{L+1}\langle\lambda_f|T^{el}_{LM}|\lambda_i\rangle \overset{k\to 0}{=} -\frac{E_f-E_i}{\hbar ck}\langle\lambda_f|M_{LM}|\lambda_i\rangle .$$

In photon-induced reactions the difference E_f-E_i between the energy eigenvalues of the nuclear states equals $\hbar ck$, the factor therefore is 1 and can be neglected. This was done in the calculation of Wachter *et al.* But this is only justified if the matrix elements are calculated using the model momentum transfer $k=k_m$. Replacing k_m by the experimental value $k=k_{ex}$ as done in this calculation as well as in those of Wachter *et al.* one must not replace E_f-E_i by $\hbar ck_{ex}$, too, because E_f and E_i are eigenvalues of the nuclear and model hamiltonian. That means the matrix elements of the Coulomb operator have to be multiplied by k_m/k_{ex} to get the Siegert's ones. Then Siegert's approximation and the full calculation agree nearly perfectly, cf. the full and the dashed lines in figs. 2 and 3.

The matrix elements of the full calculation and Siegert's approximation (if applied correctly) agree also in the limit $k\to 0$. This we consider to prove Ohta's construction of exchange currents. On the other hand, we are led to conclude that Siegert's theorem even works at momentum transfers exceeding 50 MeV/c, a fact not expected from the beginning. From the results of ref. [10]) and our explanation it becomes obvious that the use of Siegert's theorem for wave functions not derived from a hamiltonian (and therefore with unknown eigenenergies) is doubtful.

4.3. POLARIZATION OBSERVABLES IN RADIATIVE CAPTURE REACTIONS

As demonstrated in the previous subsection the large MEC contributions in the dominant $^1P_1$ E1 transition are already included in Siegert's theorem. The same holds true for the E2 transition, although here the MEC effects are very small. As the differential cross section is dominated by the E1 transition together with smaller E1–E2 admixtures [10]), there are only minor differences between the full and the Siegert calculation. Furthermore, compared to the older calculation of Wachter *et al* [10]) the corrections to the Siegert matrix elements are the same for the E1 and E2 transition. Therefore apart from the absolute strength not being covered by the experiments, the correction of the Siegert matrix elements has almost no influence on the differential radiative cross sections and the results of the older calculation remain valid in any case. As these results are discussed in ref. [10]) in great detail, we abstain from repeating them in this paper.

Searching for mesonic effects beyond Siegert's theorem one has to investigate polarization observables sensitive to magnetic transitions. At low energies the M1

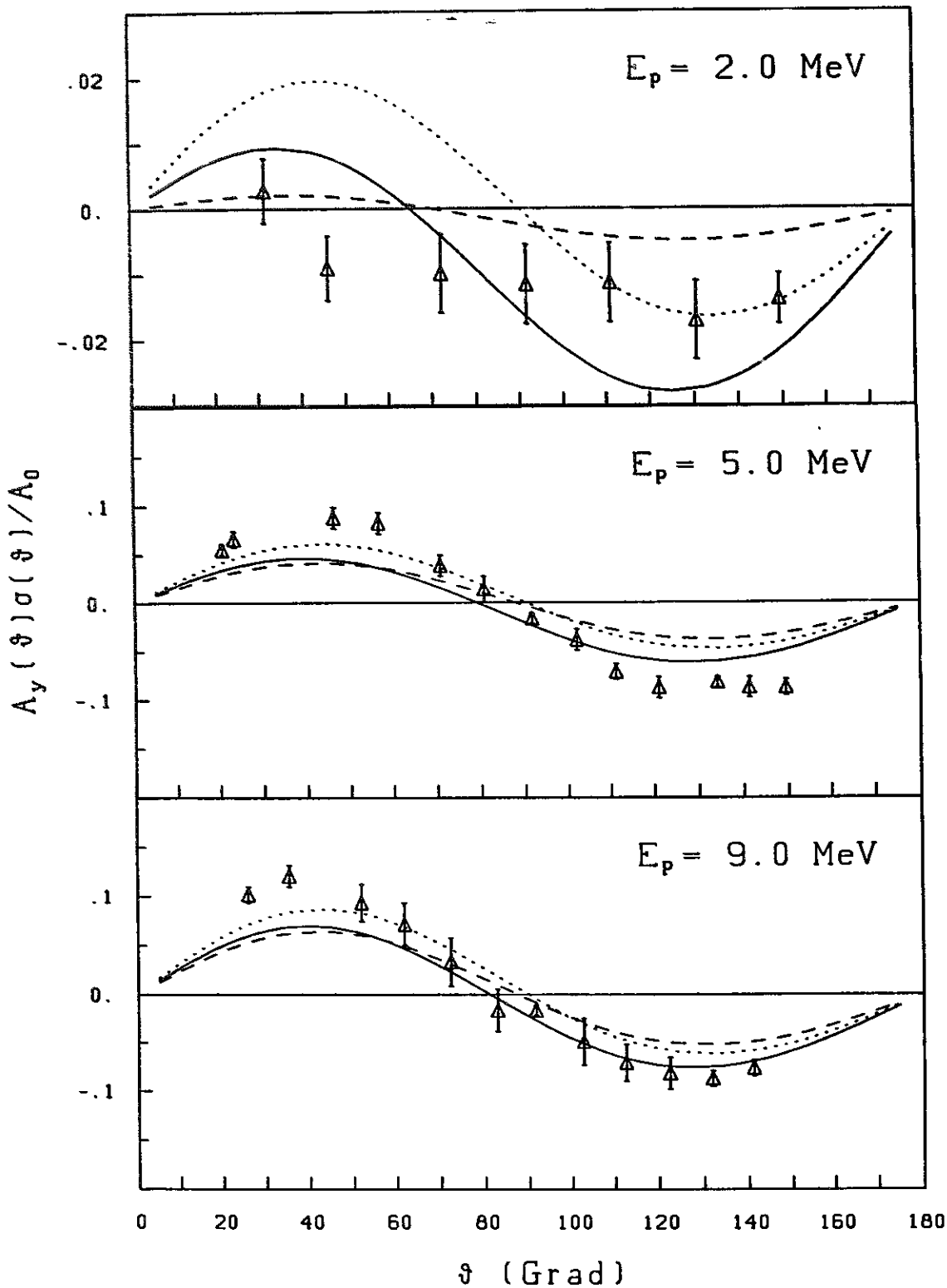

Fig. 4. Normalized analyzing powers of the reaction ^{3}He($\vec{p}$, γ)^{4}He at different proton incident energies. Full line: full calculation; dashed line: Siegert's approximation; dotted line: full calculation without M1 transition. Data: Wagenaar *et al.* (1989) [13].

contributes in a noticable way to the proton analyzing power. This is demonstrated in fig. 4 comparing the analyzing powers multiplied by the normalized differential cross section at three different proton energies with experimental results of Wagenaar *et al.* [13]). Especially at low energies there are remarkable differences between the full calculation including MEC (full line) and those using Siegert's theorem (dashed line). Firstly, the zero crossing occurs at smaller angles, secondly, the analyzing powers are larger in general if MEC are included. Both facts improve the description of the data substantially, even taking into account the large error bars at $E_p = 2$ MeV. The zero crossing depends strongly on the $^3S_1$ M1 transition as shown by the dotted line in fig. 4.

In table 2 the contributions of the different currents are listed. In contrast to the dominant E1 transition, in the $^3S_1$ nearly all the complete strength is given by the seagull current $\mathcal{O}^{se}$, whereas the convection current $\mathcal{O}^{o}$ is quite small. For the M1 convection current the direct $^3S_1$ transition is forbidden by spin selection rules; only via the weak tensor coupling to the $^5D_1$ dd channel the transition is possible. This also applies to the central current $\mathcal{O}^{ce}$, where in addition the transition via the dd channel is isospin forbidden, thus causing this current to vanish. Similarly to the $^1P_1$ the direct current $\mathcal{O}^{di}$ has different sign compared to the Seagull one, but is much smaller with respect to $\mathcal{O}^{se}$. This results from the pure tensor character of $\mathcal{O}^{di}$ in spin space allowing only for transition into the small $^5D_0$ D-wave component of the ground state.

In summary we found the analyzing power a suitable tool for studying explicit MEC effects beyond Siegert's theorem. Especially the zero crossing depends strongly on the M1 transition dominated by the two-body currents.

4.4. ELECTRODISINTEGRATION CROSS SECTIONS

At the end of this section we want to discuss the influence of MEC on the electrodisintegration cross sections in the giant-resonance energy region. As already mentioned in the Introduction we expect these influences to be small because of the dominance of the longitudinal part which is not affected by MEC. But on the

TABLE 2

Contributions of the different operators in the $^3S_1$ transition of the reaction $^3H(p, \gamma)^4He$ at $E_{c.m.} = 4.5$ MeV normalized to $\mathcal{O}^{o}$

$\mathcal{O}^{o}$	1.000
$\mathcal{O}^{s}$	−0.162
$\mathcal{O}^{ce}$	0.0
$\mathcal{O}^{se}$	6.917
$\mathcal{O}^{di,II}$	−1.501

other hand, the angular distribution of the differential cross section depends strongly on C1/E2 and C2/E1 admixtures, which are quite different in the p- and n-channels. In our previous calculation published in ref. [6]) the electric transitions were calculated using Siegert's theorem. But as in the calculation of Wachter *et al.* the difference between the energies of the nuclear states was replaced by their experiment values, which is incorrect as shown in subsect. 4.2. Therefore we will repeat this calculation here.

In fig. 5 we display the differential cross sections of the disintegration into p- and n-channels for three different energy transfers. The kinematics as well as the electron incident energy and scattering angle are the same as in ref. [6]). The full line denotes the full calculation including MEC, the dotted line those using Siegert's theorem. The dash-dotted line stands for the results of our previous calculation. The full calculation and the one using Siegert's theorem agree nearly perfectly. This means

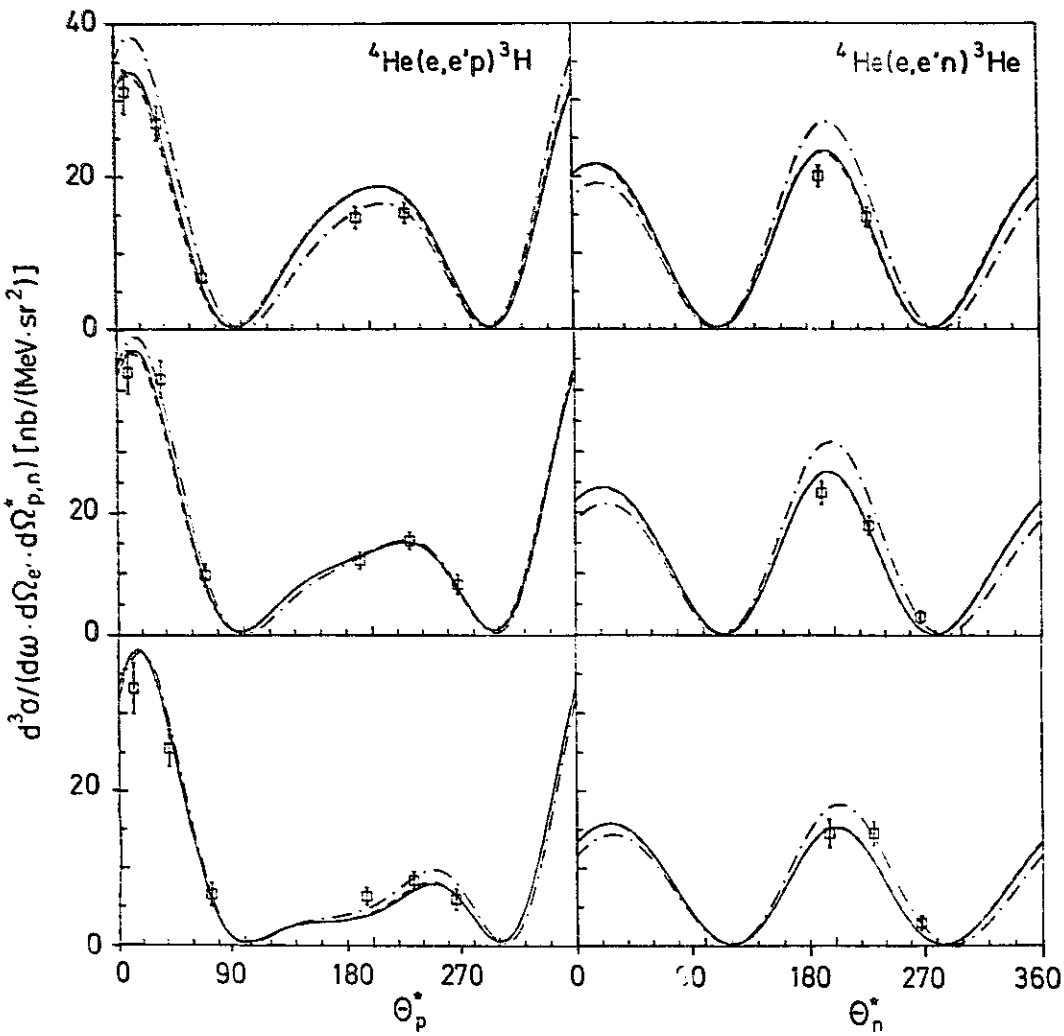

Fig. 5. Differential cross sections of the photodisintegration into p- (left-hand side) and n-channels (right-hand side) at excitation energies of 24.1 MeV (above), 27.3 MeV (middle) and 34.5 MeV (below). Data and kinematics taken from Spahn *et al.* [6]).

that Siegert's theorem works well even for momentum transfers up to 80 MeV/c. There are no influences of MEC beond this theorem, because the magnetic transitions are nearly negligible. We found some deviations between our present and our previous calculation; see the dash-dotted lines. But these deviations are quite small, because, due to the higher momentum transfer compared to photodisintegration, the error in the factor $(E_f - E_i)/\hbar ck$ is much smaller. Therefore, both the older and the present calculation agree well with the experimental data. Incidentally, the deviations vanish in the total cross sections, because the C1/E2 and C2/E1 admixtures no longer contribute and the total cross section is then completely dominated by longitudinal transitions.

5. Conclusion

In the framework of the RRGM we calculated observables of ^{4}He photo- and electrodisintegration as well as those of the corresponding radiative-capture reactions, for the first time taking into account MEC explicitly. We used a consistent approach of Ohta [18,19]) based on gauge invariance to derive these currents from our semi-realistic NN potential. This means our currents fulfill the continuity equation. We compared our results to those obtained by applying the usual Siegert's theorem.

We were able to describe simultaneously the most recent experimental photodisintegration cross sections, the polarization observables of the corresponding radiative-capture reaction as well as the electrodisintegration cross sections. Therefore, we see no need for a genuine charge-symmetry breaking in the p- and n-channels.

In general we found large MEC contributions to the observables in the photon-induced reactions. In the photodisintegration 30–40% if the dominant $^1P_1$ strength is caused by MEC. In the $^3S_1$ M1 transitions MEC are even the dominant part. Especially the crossing through zero of the analyzing powers is very sensitive to the M1 contribution and therefore on MEC. The electrodisintegration reactions, however, are much more insensitive because they are dominated by the longitudinal part of the electromagnetic interaction.

We explained the large discrepancies between the full calculation including MEC and older ones using Siegert's theorem to be caused by an incorrect application of this theorem. By a consistent use of Siegert's theorem, however, we found excellent agreement even for quite large momentum transfers. Considering all this we question calculations using fitted wave functions and experimental energies together with Siegert's theorem.

The semi-realistic NN potential is not without flaws, in spite of the apparent success of our calculation. Due to the weak repulsive core the calculation cannot be extended beyond center-of-mass energies of about 30 MeV, thus the recent NIKHEF (e, e'X) experiments [34]) cannot be covered by the present calculations. Furthermore, the missing D-wave admixtures in the fragments do not allow one to answer the question of internal E2 transitions contributing to the dd radiative capture

at low energies [35]). Finally, the too low dd threshold shifts the small channel-coupling effects towards too low energy; i.e. the present calculation cannot be improved on further.

A realistic potential, as for instance the Bonn potential, allows one to cure all the above problems; hence, such calculations are highly desirable in spite of their tremendous technical difficulties. Such types of calculations are under way.

The authors are indebted to J.L. Friar for various discussions on Siegert's theorem.

Appendix A

CALCULATION SCHEME OF THE MATRIX ELEMENTS IN COORDINATE SPACE

In this appendix we indicate the explicit calculation of the matrix elements of the form given in eq. (56). Since the derivation parallels those of the norm matrix elements, we follow closely ref. [30]) and discuss only the differences between both evaluations. First one uses the multipole expansion of the plane wave to rewrite $j_L(kr)\,Y_{LM}(\Omega_r)$ in terms of plane waves [24]),

$$j_L(kr)\,Y_{LM}(\Omega_r)=\frac{1}{4\pi i^L}\int \mathrm{d}\Omega\; Y_{LM}(\Omega_k)\,\mathrm{e}^{i\boldsymbol{k}\cdot\boldsymbol{r}}\,. \tag{A.1}$$

Instead of eq. (4.1) of ref. [30]) we have to solve

$$I=(-1)^{m_1+\cdots+m_{n_{c_\ell}-1}}\Gamma_{l_1,m_1,\ldots,l_z,m_z}\,, \tag{A.2}$$

$$\begin{aligned}\Gamma_{l_1,m_1,\ldots,l_z,m_z}=&\frac{1}{4\pi i^L}\int \mathrm{d}\Omega\; Y_{LM}(\Omega_k)\int \mathrm{d}^3s_1\ldots\mathrm{d}^3s_{A-1}\\ &\times\exp\left\{-\sum_{\nu,\nu'=1}^{A-1}\rho_{\nu\nu'}(\not\mu)\boldsymbol{s}_\nu\cdot\boldsymbol{s}_{\nu'}+i\sum_{\nu=1}^{A-1}[(\tfrac{1}{2}-v)\eta_{\nu i}(\not\mu)+(\tfrac{1}{2}+v)\eta_{\nu j}(\not\mu)]\boldsymbol{k}\cdot\boldsymbol{s}_\nu\right\}\\ &\times\prod_{n=1}^{z}\mathcal{Y}_{l_n m_n}(\boldsymbol{Q}_n)\,,\end{aligned} \tag{A.3}$$

with

$$z=n_{c_\ell}+n_{c_r}+N_0-2\,,$$

$$\boldsymbol{r}_i=\sum_{\nu=1}^{A-1}\eta_{\nu i}(\not\mu)\boldsymbol{s}_\nu\,,$$

$$\boldsymbol{Q}_n=\sum_{\nu=1}^{A-1}\xi_{\nu n}(\not\mu)\boldsymbol{s}_\nu\,.$$

Similar to ref. [30]) we introduce the generating function of the integrals and find exactly the same connection (4.16). Transforming the gaussians into a diagonal form

by the transformation matrix T and using the standard method of completing squares finally we arrive at

$$\begin{aligned}\Gamma_{l_1,m_1,\ldots,l_z,m_z} = & \frac{1}{4\pi i^L}\prod_{\nu=1}^{A-1}\left(\frac{\pi}{\beta_\nu}\right)^{3/2}\prod_{\tilde{n}=1}^{z}\left(\frac{l_{\tilde{n}}!}{c_{l_{\tilde{n}}m_{\tilde{n}}}}\right)\\ & \times\exp\{-[(\tfrac{1}{2}-v)^2\alpha_{ii}+2(\tfrac{1}{4}-v^2)\alpha_{ij}+(\tfrac{1}{2}+v)^2\alpha_{jj}]k^2\}\\ & \times\sum_{\substack{g_{nn'}\\ h_{nn'},k_{nn'}}}\prod_{n<n'}^{z}(-1)^{h_{nn'}+k_{nn'}}2^{g_{nn'}}\frac{\sigma_{nn'}^{g_{nn'}+h_{nn'}+k_{nn'}}}{g_{nn'}!h_{nn'}!k_{nn'}!}\\ & \times\sum_{d_r,e_r}\prod_{r=1}^{z} i^{d_r}\frac{c_{d_re_r}}{d_r!}[(\tfrac{1}{2}-v)\gamma_{ir}+(\tfrac{1}{2}+v)\gamma_{jr}]^{d_r}k^{d_r}\\ & \times\int \mathrm{d}\Omega\, Y_{LM}(\Omega_k)Y_{d_re_r}(\Omega_k)\,, \end{aligned}\tag{A.4}$$

with

$$\sigma_{nn'}=\sum_{\lambda=1}^{A-1}\frac{P_{n\lambda}P_{n'\lambda}}{\beta_\lambda},\qquad \alpha_{ij}=\sum_{\lambda=1}^{A-1}\frac{\omega_{i\lambda}\omega_{j\lambda}}{4\beta_\lambda},$$

$$\gamma_{in}=\sum_{\lambda=1}^{A-1}\frac{\omega_{i\lambda}P_{n\lambda}}{2\beta_\lambda},\qquad \omega_{i\lambda}=\sum_{\nu=1}^{A-1}\eta_{\nu i}T_{\lambda\nu},$$

which corresponds to eq. (4.24). The additional spherical harmonics originate from the expansion of the exponential linear in k. In contrast to ref. [30]) the summations are governed by new rules, given below:

$$g_{nn'},\ h_{nn'},\ k_{nn'},\ d_r\geqslant 0,\qquad |e_r|\leqslant d_r\quad\text{integer},\tag{A.5}$$

$$l_n=d_n+\sum_{\substack{n'\\ n'>n}}^{z}g_{nn'}+h_{nn'}+k_{nn'}+\sum_{\substack{n'\\ n'<n}}^{z}g_{n'n}+h_{n'n}+k_{n'n},\tag{A.6}$$

$$m_n=e_n+\sum_{\substack{n'\\ n'>n}}^{z}(k_{nn'}-h_{nn'})+\sum_{\substack{n'\\ n'<n}}^{z}(h_{n'n}-k_{n'n})\,.\tag{A.7}$$

The integration over the spherical harmonics gives two additional constraints

$$\sum_{n=1}^{z}d_n+L\quad\text{even},\tag{A.8}$$

$$\sum_{n=1}^{z}e_n=M,\tag{A.9}$$

and parity conservation leads to another one

$$\sum_{n=1}^{z}l_n\begin{Bmatrix}\text{even}\\ \text{odd}\end{Bmatrix}\Rightarrow\sum_{n=1}^{z}d_n\begin{Bmatrix}\text{even}\\ \text{odd}\end{Bmatrix}.\tag{A.10}$$

Eq. (A.4) together with eqs. (A.5)-(A.10) enable us to solve the matrix elements of all operators without gradients analytically.

In contrast to all other operators the convection current contains a gradient:

$$\tilde{I} = \sum_{M'\nu} (L'\,M'\,1\,\nu|L\,M)\langle\alpha_f, l_f, m_f|\not{p} j_{L'}(kr')\,Y_{L'M'}(\Omega_{r'})\nabla_\nu|\alpha_i, l_i, m_i\rangle\,. \quad \text{(A.11)}$$

The calculation of these matrix elements is quite similar to those without gradients [30]). Since the evaluation is straightforward but somewhat lengthy, we only give the result.

$$\tilde{I} = (-1)^{m_1+\cdots+m_{n_{c_f}-1}}\tilde{\Gamma}_{l_1,m_1,\ldots,l_n,m_n}\,, \quad \text{(A.12)}$$

$$\tilde{\Gamma}_{l_1,m_1,\ldots,l_n,m_n} = \sum_{M'\nu} (L'\,M'\,1\,\nu|L\,M) \sum_{n=1}^{\tilde{n}} [(2-\sqrt{2})|\nu|-2]$$

$$\times\, \Lambda_{ni}\frac{c_{l_n-1\,m_n+\nu}}{c_{l_n m_n}}\, l_n\Gamma_{l_1,m_1,\ldots,l_n-1,m_n+\nu,\ldots,l_n,m_n}\,, \quad \text{(A.13)}$$

with

$$\Lambda_{ni} = \sum_{\lambda=1}^{A-1}\eta_{\lambda i}\left(\xi_{n\lambda}\Theta(n-n_{c_f}+1) - \sum_{\gamma,\mu}^{A-1}[\rho'_{\mu\lambda}(\not{p})+\rho'_{\lambda\mu}(\not{p})]\Upsilon_{\mu\lambda}\frac{P_{n\gamma}}{2\beta_\gamma}\right). \quad \text{(A.14)}$$

The $\rho'_{\lambda\mu}(\not{p})$ are defined like the $\rho_{\nu\nu'}(\not{p})$ from eq. (A.3), but only the width parameters of the right-hand side are taken into account. $\Theta(n)$ is the usual step function with $\Theta(n)=1$ for $n>0$ and 0 otherwise.

Appendix B

^{4}He BOUND-STATE WAVE FUNCTION

In this appendix we give the explicit form of the ^{4}He ground-state wave function. In the following Ξ^S denotes the spin-isospin function coupled to total spin S. The normalized Jacobi coordinate between the fragments in the ^{3}H-p and the ^{3}He-n configuration is written as s_3, that between the deuterons as s'_3.

$$|\psi\rangle^{0+} = \mathcal{A}_4|\bar{\psi}\rangle^{0+}\,,$$

$$|\bar{\psi}\rangle^{0+} = \varphi^3\mathrm{H}\times\left(\sum_{m=1}^{4} c_m \exp(-\delta_m s_3^2)\right)\times[\mathcal{Y}_0(s_3)\otimes\Xi^0]^0$$

$$+\varphi^3\mathrm{He}\times\left(\sum_{m=5}^{8} c_m \exp(-\delta_m s_3^2)\right)\times[\mathcal{Y}_0(s_3)\otimes\Xi^0]^0$$

$$+\varphi^2\mathrm{H}\times\varphi^2\mathrm{H}\times\left(\sum_{m=8}^{11} c_m \exp(-\delta_m s_3'^2)\right)\times[\mathcal{Y}_0(s'_3)\otimes\Xi^0]^0$$

$$+\varphi^2\mathrm{H}\times\varphi^2\mathrm{H}\times\left(\sum_{m=11}^{15} c_m \exp(-\delta_m s_3'^2)\right)\times[\mathcal{Y}_2(s'_3)\otimes\Xi^2]^0\,.$$

TABLE 3

Radial-width parameters and superposition coefficients for the ^{4}He bound-state wave function in fm^{-2}

	m	$10^3 c_m$	δ_m		m	$10^3 c_m$	δ_m
^{3}H-p	1	−77.91	1.2719	^{2}H-d	9	1.813	0.4447
	2	208.3	0.4447		10	−0.256	0.1690
	3	−1.88	0.1690		11	−0.0188	0.05
	4	−0.6009	0.05		12	8.262	0.4447
					13	0.8349	0.1690
^{3}He-n	5	−78.36	1.2719		14	0.03698	0.08
	6	212.9	0.4447		15	−0.006726	0.05
	7	−5.802	0.1690				
	8	−0.1854	0.05				

The coefficients c_m and δ_m are given in table 3. The functions φ are given by [36,37])

$$\varphi^{^3\mathrm{H}} = \varphi^{^3\mathrm{He}} = \sum_{n=1}^{2} d_n \exp\left(-\tfrac{1}{3}\beta_n \sum_{1<i<j}^{3} (r_i - r_j)^2\right),$$

with $\beta_1 = 0.0843$, $\beta_2 = 0.2393$, $d_1 = 0.0184$ and $d_2 = 0.1428$ and

$$\varphi^{^2\mathrm{H}} = \sum_{n=1}^{2} d_n \exp\left[-\tfrac{1}{2}\beta_n (r_i - r_j)^2\right],$$

with $\beta_1 = 0.0403$, $\beta_2 = 0.3204$, $d_1 = 0.1492$ and $d_2 = 0.5320$.

References

1) G.A. Miller, B.M.K. Nifkens and I. Slaus, Phys. Reports **194** (1990) 1
2) B.L. Berman, D.D. Faul, P. Meyer and D.L. Olson, Phys. Rev. **C22** (1980) 2273
3) L. Ward, D.R. Tilly, D.M. Skopik, N.R. Robertson and H.R. Weller, Phys. Rev. **C24** (1981) 317
4) C.K. Malcom, D.V. Webb, Y.M. Shin and D.M. Skopik, Phys. Lett. **B47** (1973) 433
5) J.D. Irish, R.G. Johnson, B.L. Berman, B.J. Thomas, G.K. McNeill and J.W. Jury, Can. J. Phys. **53** (1975) 802
6) M. Spahn, Th. Kihm, K.T. Knöpfle, J. Friedrich, N. Voegler, Ch. Schmitt, V.H. Walther, M. Unkelbach and H.M. Hofmann, Phys. Rev. Lett. **63** (1989) 1574
7) R. Bernabei, A. Chisholm, S. d'Angelo, M.P. de Pascale, P. Picozza, C. Schaerf, B. Belli, L. Casano, A. Incicchitti, D. Prosperi and B. Girolami, Phys. Rev. **C38** (1988) 1990
8) G. Feldman, M.J. Balbes, L.H. Kramer, J.Z. Williams, H.R. Weller and D.R. Tilly, Phys. Rev. **C42** (1990) 1167
9) D. Halderson and R.J. Philpott, Nucl. Phys. **A359** (1981) 365
10) B. Wachter, T. Mertelmeier and H.M. Hofmann, Phys. Rev. **C38** (1988) 1139
11) J. Dubach, J.H. Koch and T.W. Donnelly, Nucl. Phys. **A271** (1976) 279
12) A.J.F. Siegert, Phys. Rev. **52** (1937) 787
13) D.J. Wagenaar, N.R. Robertson, H.R. Weller and D.R. Tilly, Phys. Rev. **C39** (1989) 352
14) K.-M. Schmitt and H. Arenhövel, Few Body Syst. **7** (1989) 95
15) R. Machleidt, K. Holinde and Ch. Elster, Phys. Reports **149** (1987) 1
16) D.O. Riska, Phys. Scr. **31** (1985) 471
17) A. Buchmann, W. Leidemann and H. Arenhövel, Nucl. Phys. **A443** (1985) 726
18) K. Ohta, Nucl. Phys. **A495** (1989) 564

19) K. Ohta, Phys. Rev. C39 (1989) 2302
20) T. de Forest and J.D. Walecka, Adv. in Phys. 15 (1966) 1
21) H. Überall, Electron scattering from complex nuclei, part A and B (Academic Press New York, 1971)
22) T.W. Donnelly and J.D. Walecka, Annu. Rev. Nucl. Sci. 25 (1975) 329
23) T. Mertelmeier and H.M. Hofmann, Nucl. Phys. A459 (1986) 387
24) A.R. Edmonds, Angular momentum in quantum mechanics (Princeton Univ. Press, Princeton, 1960)
25) J.M. Blatt and V.W. Weisskopf, Theoretical nuclear physics (Wiley, New York, 1952)
26) H. Arenhövel, Z. Phys. A302 (1981) 25
27) B. Mosconi and P. Ricci, Phys. Rev. C36 (1987) 60
28) H.H. Hackenbroich, Z. Phys. 231 (1970) 216
29) H.H. Hackenbroich, Reactions involving light nuclei, Symp. on the present status and novel development in the nuclear many-body problem, Rome, Editrice Compositori (1973)
30) H.M. Hofmann, Lecture Notes in Physics 273 (1987) 243
31) B. Wachter, T. Mertelmeier and H.M. Hofmann, Phys. Lett. B200 (1988) 246
32) W.E. Meyerhof, M. Suffert and W. Feldman, Nucl. Phys. A148 (1970) 211
33) A.N. Gorbunov, Phys. Lett. B27 (1968) 436
34) R. Ent, H.P. Blok, J.F.J. van den Brand, H.J. Bulten, E. Jans L. Lapikás and H. Morita, Phys. Rev. Lett. 67 (1991) 18
35) J. Piekarewicz and S.E. Koonin, Phys. Rev. C36 (1987) 875
36) H. Stöwe and W. Zahn, Nucl. Phys. A289 (1977) 317
37) H. Stöwe and W. Zahn, Z. Phys. A286 (1978) 173